

# **Exhibit 32**



ELSEVIER

Contents lists available at ScienceDirect

## Continental Shelf Research

journal homepage: [www.elsevier.com/locate/csr](http://www.elsevier.com/locate/csr)

## Research papers

## Sediment deposition from tropical storms in the upper Chesapeake Bay: Field observations and model simulations

Cindy M. Palinkas<sup>a,\*</sup>, Jeffrey P. Halka<sup>b</sup>, Ming Li<sup>a</sup>, Lawrence P. Sanford<sup>a</sup>, Peng Cheng<sup>a</sup><sup>a</sup> Horn Point Laboratory, University of Maryland Center for Environmental Science, PO Box 775, Cambridge, MD 21613, USA<sup>b</sup> Maryland Geological Survey, 2300 St. Paul Street, Baltimore, MD 21218, USA

## ARTICLE INFO

## Article history:

Received 31 August 2012

Received in revised form

6 September 2013

Accepted 12 September 2013

Available online 20 September 2013

## Keywords:

Flood-sediment deposition

Sediment resuspension

Tropical storms

Sediment transport modeling

## ABSTRACT

Episodic flood and storm events are important drivers of sediment dynamics in estuarine and marine environments. Event-driven sedimentation has been well-documented by field and modeling studies, though both techniques have inherent limitations. A unique opportunity to integrate field observations and model results was provided in late August/early September 2011 with the passage of Hurricane Irene and Tropical Storm Lee in the Chesapeake Bay region. Because these two storms occurred within a relatively short period of time, both are potentially represented in the sediment record obtained during rapid-response cruises in September and October 2011. Associated sediment deposits were recognized in cores using classic flood-sediment signatures (fine grain size, uniform <sup>7</sup>Be activity, physical stratification in x-radiographs) and were found to be < 4 cm, thickest in the upper Bay. A coupled hydrodynamic-sediment transport model is used to simulate the sediment plume and sediment deposition onto the seabed. The predicted deposition thickness for TS Lee is in general agreement with the observational estimates. One exception with physical stratification but no <sup>7</sup>Be activity appears to be due to extreme wave activity during Hurricane Irene. Integration of observations and modeling in this case greatly improved understanding of the transport and fate of flood sediments in the Chesapeake Bay.

© 2013 Elsevier Ltd. All rights reserved.

## 1. Introduction

Episodic flood and storm events are important drivers of sediment dynamics in estuarine and marine environments. Among others, these short-term (generally a few days) depositional and erosional events affect such properties as seabed stability and strength, the building of the stratigraphic record, and the local biological community (Gallucci and Netto, 2004; Sommerfield et al., 1999; Wheatcroft and Drake, 2003). Event-driven sedimentation has been well-documented by field and modeling studies, yet there are inherent limitations in both techniques. For example, field observations are useful for documenting the mass and extent of flood deposition but typically have poor spatial coverage and are unable to resolve thin (mm-scale) deposits (Allison et al., 2000; Dail et al., 2007; Palinkas et al., 2005; Wheatcroft et al., 2006). Models can be used to overcome these challenges, but they require validation and rely on assumptions of particle delivery and size-class characteristics, among other parameters (Bever et al., 2009; Friedrichs and Scully, 2007). Field results and model simulations of sedimentary processes during hurricanes have been integrated in previous studies to understand the creation and

preservation of sedimentary fabric (Bentley et al., 2002, 2006), evaluate differences in sediment resuspension processes during events spaced closely in time (Dickey et al., 1998), and compare modern storm-bed deposition to events in the ancient sedimentary record (Keen et al., 2006), among other applications.

A unique opportunity to integrate field observations and model results in the Chesapeake Bay region was provided in late August/early September 2011 with the passage of Hurricane Irene and the remnants of Tropical Storm (TS hereafter) Lee. These storms differed in their timing, track, and impact on the Bay region—Hurricane Irene was primarily a wind/sediment resuspension event, whereas TS Lee was a hydrological/sediment deposition event. Because these two storms occurred within a relatively short period of time, both are potentially represented in the sediment record obtained by coring during rapid-response cruises in September and October 2011. In contrast, model runs can focus on dynamics from individual storms, such as resuspension during Hurricane Irene and deposition following TS Lee. The primary focus of this study is on TS Lee, not only because of the large amounts of sediment deposition expected and concern about associated potential ecological damage like that following Tropical Storm Agnes in 1972 (Schubel and Hirschberg, 1978), but also because the model used in this study (see Section 2) does not simulate waves and hence will underestimate bottom stress and resuspension during Hurricane Irene.

\* Corresponding author. Tel.: +1 410 221 8487.

E-mail address: [cpalinkas@umces.edu](mailto:cpalinkas@umces.edu) (C.M. Palinkas).

The objectives of this study are to: (1) estimate the thickness and extent of sediment deposited in upper Chesapeake Bay following Hurricane Irene and TS Lee with field observations and model simulations, and (2) integrate field and model techniques to improve understanding of flood-sediment transport and fate in the Bay.

### 1.1. Hurricane Irene and Tropical Storm Lee description

Hurricane Irene (formed and dissipated on 21 and 28 August 2011, respectively) passed through the Chesapeake Bay region on 27–28 Aug, tracking east of the Bay and following the mid-Atlantic coast. Due to this track, maximum rainfall totals were highest on the eastern shore of the Bay, where tributaries typically have small watersheds ( $\sim 100$ – $1000 \text{ km}^2$ ) and deliver little fine sediment to the Bay due to their relatively low relief and sandy sediments (Langland and Cronin, 2003). Elevated discharge is generally short-lived for these tributaries and little fine-sediment is delivered to Chesapeake Bay. For example, the Choptank River, one of the largest eastern-shore tributaries (watershed area  $1780 \text{ km}^2$ ), had record discharge after Hurricane Irene ( $251.3 \text{ m}^3/\text{s}$ ; [www.water.usgs.gov](http://www.water.usgs.gov)) that was two orders of magnitude greater than the average discharge ( $3.7 \text{ m}^3/\text{s}$ ; Yarbro et al., 1983); however, discharge had returned to previous baseflow levels within a few days. The Susquehanna River and tributary rivers on the Bay's western shore tend to have larger drainage basins with steeper gradients than those of the Coastal Plain and eastern shore, and as a result, they deliver greater amounts of sediment to the Chesapeake Bay estuarine system (Langland and Cronin, 2003). In particular, the Susquehanna River, the largest river discharging into Chesapeake Bay, delivers about half the freshwater entering the upper Bay (Schubel, 1972) and  $2 \times 10^6 \text{ t}$  of sediment annually (Langland and Cronin, 2003). The western-shore tributaries rivers experienced increased river discharge associated with Hurricane Irene; however, maximum discharge ( $2635 \text{ m}^3/\text{s}$  on 29 August 2011 for the Susquehanna River) was well below flood thresholds ( $\sim 8500 \text{ m}^3/\text{s}$  for the Susquehanna; [www.water.usgs.gov](http://www.water.usgs.gov)). Additionally, these tributaries (except the Susquehanna) discharge into tributary estuaries before entering the Bay and serve as effective sediment traps, even during high-flow events (e.g., Tropical Storm Agnes; Nichols, 1977). Indeed, satellite images taken after the passage of Hurricane Irene (Fig. 1a) show that most of the turbidity is confined within tributaries.

The remnants of Tropical Storm Lee (formed and dissipated on 2 and 5 September 2011, respectively) passed through the Chesapeake Bay watershed 7–11 Sept. Unlike Hurricane Irene, heavy precipitation was focused largely on the Susquehanna River watershed and extended from the upper western shore of Maryland northward to New York. The heavy precipitation associated with TS Lee resulted in the second (behind Tropical Storm Agnes in 1972) highest recorded Susquehanna River discharge. Discharge peaked at  $22,002 \text{ m}^3/\text{s}$  on 9 September 2011 and was so high that it exceeded the predicted scour threshold for sediments behind the Conowingo Dam ( $11,320 \text{ m}^3/\text{s}$ ;  $400,000 \text{ ft}^3/\text{s}$ ) for a total of 3 days during the event. Approximately  $4 \times 10^6 \text{ t}$  of sediment were scoured from behind the Dam and subsequently transported into the upper Chesapeake Bay (<http://chesapeake.usgs.gov/featuresedimentscourconowingo.html>), along with newly eroded watershed sediment. Various estimates have been generated for the amount of sediment delivered to the Chesapeake Bay associated with TS Lee, ranging from  $6.7$  to  $19.0 \times 10^6 \text{ t}$  (Cheng et al., 2013; Hirsch, 2012),  $\sim 4$ – $10$  times greater than the annual load of the Susquehanna. Satellite images taken after the storm show a dramatic sediment plume in Chesapeake Bay (Fig. 1b).

To put these events into a broader context, the highest river flow recorded to date for the Susquehanna River occurred during

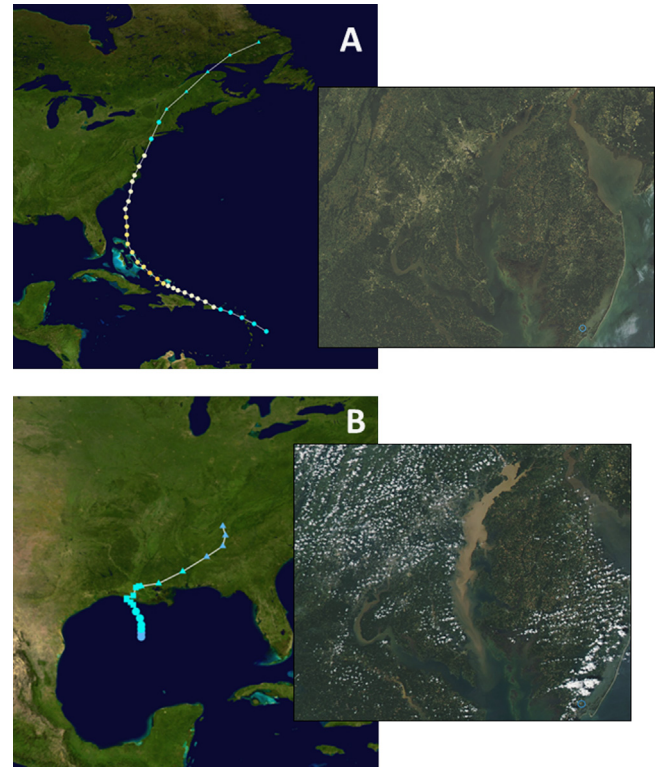


**Fig. 1.** Storm tracks (left) and satellite images (right; focused on Chesapeake Bay) after the passage of (A) Hurricane Irene and (B) the remnants of Tropical Storm Lee. Storm tracks are from [http://commons.wikimedia.org/wiki/file:Irene\\_2011\\_track.png](http://commons.wikimedia.org/wiki/file:Irene_2011_track.png) and [http://commons.wikimedia.org/wiki/file:Lee\\_2011\\_track.png](http://commons.wikimedia.org/wiki/file:Lee_2011_track.png), respectively. Symbols represent the storm type (circle=tropical cyclone, square=subtropical cyclone, triangle=extratropical cyclone); colors indicate the intensity on the Saffir-Simpson Hurricane Scale (blue=tropical depression, aqua=tropical storm, pale yellow=category 1, yellow=category 2, orange=category 3). Both satellite images are from <http://lance-modis.eosdis.nasa.gov>. Satellite image after Irene is from the Terra sensor, taken on 30 Aug 2011; satellite image after Lee is from the Aqua sensor taken on 13 Sept 2011. After Irene, turbidity is mostly restricted to tributaries, with some resuspension evident. After Lee, turbidity extends throughout much of the Chesapeake Bay from the Susquehanna River plume. (For interpretation of the references to color in this figure legend, the reader is referred to the web version of this article.)

TS Agnes in 1972 ( $31,998 \text{ m}^3/\text{s}$ ; <http://www.water.usgs.gov>). TS Agnes discharged  $31 \times 10^6 \text{ t}$  of suspended sediments into Chesapeake Bay (Schubel, 1976) and delivered sufficient nutrients and organic matter to support elevated plankton production for several years (Loftus and Seliger, 1976). Core samples collected after TS Agnes showed a 20–30-cm thick sediment deposit in upper Chesapeake Bay observed in x-radiographs (Zabawa and Schubel, 1974). In addition, TS Agnes destroyed over 60% of the submerged aquatic vegetation (SAV) in the upper Bay (Kerwin et al., 1976), highlighting the potential of storm events to cause ecological damage.

## 2. Methods

### 2.1. Monitoring data

We did not directly collect data on winds, waves, and river flow during this study, but rather made use of data collected by several ongoing monitoring efforts (see Fig. 2 for station locations). Wind data are available from Thomas Point Light from the NOAA National Data Buoy Center ([www.ndbc.noaa.gov](http://www.ndbc.noaa.gov)). The US Geological Survey maintains several gauges on the Susquehanna River ([www.water.usgs.gov](http://www.water.usgs.gov)); this study uses data from the gauge at

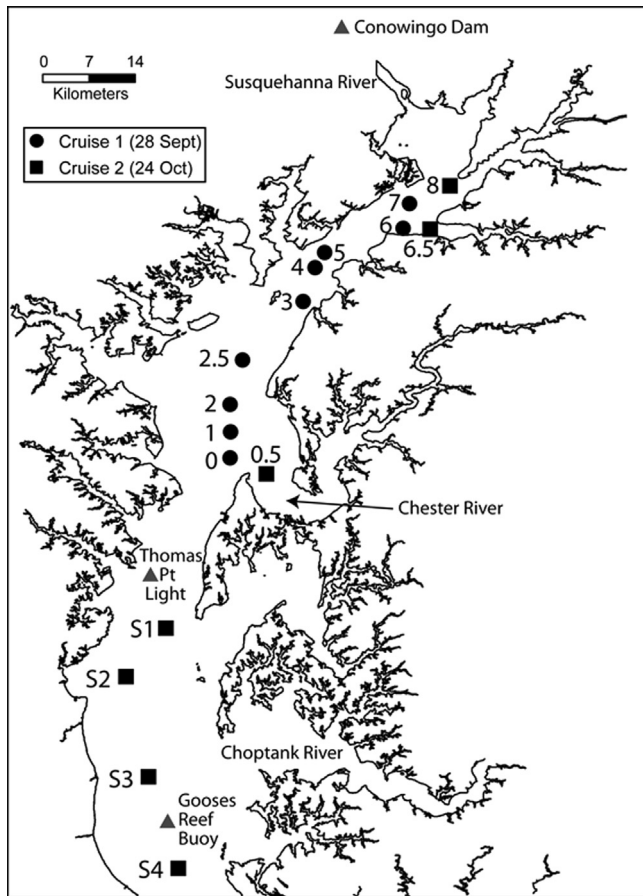


**Fig. 2.** Map of Chesapeake Bay showing coring locations with station numbers. Stations in the text and Table 1 refer to stations as “LeeN,” where N is the station number. Circles and squares denote stations cored on the first and second sampling cruises, respectively. Triangles represent other locations mentioned in the text.

Conowingo Dam. Lastly, wave and suspended-sediment data are available at Gooses Reef from the Chesapeake Bay Interpretative Buoy System (CBIBS; [buoybay.noaa.gov](http://buoybay.noaa.gov)).

## 2.2. Field observations and laboratory analyses

Two rapid-response cruises were organized following the passage of the remnants of TS Lee. The first cruise occurred on 28 September 2011, ~3 weeks after peak discharge of the Susquehanna River and focused on the upper Chesapeake Bay. Several stations on this cruise were purposefully co-located with those sampled by [Zabawa and Schubel \(1974\)](#) to facilitate comparisons of our observations with those taken after Hurricane Agnes in 1972. The second cruise occurred ~1 month later, on 24 October 2011, extending observations northward and southward of our initial stations. A total of 16 gravity cores were collected ([Fig. 2](#)); intact cores were returned to the Maryland Geological Survey, where x-radiographs were taken within 1–2 days.

Cores were subsequently transferred to Horn Point Laboratory and sectioned vertically into 1-cm increments for further analysis. Samples were prepared for grain-size measurements by disaggregation in a sodium metaphosphate solution and placed in an ultrasonic bath prior to analysis. These subsamples were then wet-sieved at 64  $\mu\text{m}$  to separate the mud (< 64  $\mu\text{m}$ ) and sand (> 64  $\mu\text{m}$ ) component. The mud fraction was then placed into a Sedigraph 5120 grain-size analyzer to determine the grain-size distribution.

The 1-cm increment samples were also analyzed for the naturally occurring radioisotope  $^7\text{Be}$  by gamma spectroscopy of

the 477.7 keV photopeak. These subsamples were dried, ground, and placed into identical 60-mL counting jars, taking care to ensure consistent counting geometry. Samples were counted for ~24 h in germanium detectors that were calibrated following [Larsen and Cutshall \(1981\)](#), using commercially available standards. Activities were decay-corrected to the time of sample collection and are reported in dpm/g.

$^7\text{Be}$  (half-life 53.3 d) is an ideal radionuclide for investigating event sediment deposition due to its relatively short half-life and atmospheric source.  $^7\text{Be}$  is produced by cosmic-ray spallation of nitrogen and oxygen in the atmosphere, delivered to Earth’s surface through precipitation (wet and dry), and adsorbs onto terrestrial particles that are then eroded and transported to the aquatic environment ([Baskaran and Santschi, 1993](#); [Olsen et al., 1986](#)). The presence of  $^7\text{Be}$  in the seabed indicates that the material had been on land within 4–5 half-lives (the assumed limit of detectability) or ~200 d. For seabed sediment to have detectable  $^7\text{Be}$ , watershed sediment must be rapidly eroded and delivered to the aquatic environment without prolonged storage in the drainage basin, such as typically occurs during large flood events. Previous studies have shown the flood sediment can be recognized in cores by several signatures—relatively uniform  $^7\text{Be}$  activities, finer grain size and physical stratification in x-radiographs ([Palinkas et al., 2005](#); [Sommerfield et al., 1999](#)).

## 2.3. Wave resuspension model

Wave-induced bottom stresses in the mid-Bay at the peak of Hurricane Irene were estimated using procedures described by [Sanford \(1994\)](#). Briefly, near-bottom velocity fluctuations were estimated from significant wave height, wave period, and water depth using linear wave theory. Characteristic water depths were evaluated along an east–west lateral transect across the Bay at core location LeeS3. Wave bottom friction coefficients were estimated using a numerical approximation of the Jonsson wave friction factor diagram (e.g., [Madsen, 1976](#)), which allows for the complete range of wave, roughness, and Reynolds number dependence of the drag coefficient. The present estimates assumed an equivalent bottom roughness length of 0.1 mm appropriate for silt-dominated bottom sediments, a significant wave height of 2.5 m, and a wave period of 5.5 s, based on the waves observed at Gooses Reef during the peak of Irene on 28 August 2011. Because significant portions of the lateral transect were in shallow enough water to cause depth-limited wave breaking, wave heights were limited to 0.78 times the water depth for the purposes of stress estimation. Estimates of the critical stresses for erosion of mid-Bay silts range from 0.12 Pa at the sediment surface to 0.3 Pa at about 1 mm sediment depth ([Sanford, 2006](#)), based on nearby sediment erodibility experiments in May 2002.

## 2.4. Sediment transport model

A coupled hydrodynamic-sediment-transport model was used to study the impacts of TS Lee on sediment transport and deposition in Chesapeake Bay. The hydrodynamic model is based on ROMS (Regional Ocean Modeling System; [Haidvogel et al., 2000](#)) and has been previously validated by [Li et al. \(2005, 2006\)](#) and [Zhong and Li \(2006\)](#). The model domain covers the main stem of the Bay, 8 major tributaries and a part of the coastal ocean to facilitate free exchange across the Bay mouth. The model has 240  $\times$  160 horizontal grids and 20 vertical layers. The horizontal grid resolution is about 500 m. It is forced by freshwater inflows at river heads, tidal and non-tidal flows at the offshore boundary, and winds and heat exchanges across the water surface. The model integration starts from 1 September 2011 and ends on 30 June

2012 and is initiated with the outputs from a hindcast simulation from 1 January 2010 to 31 August 2011.

The sediment-transport model is based on that developed by Warner et al. (2008) and simulates sediment erosion, suspension, transport, and deposition. The sediment is introduced into the model domain through rivers and erosion from the seabed. The Susquehanna River is the only source of fluvial sediment in the model, as it is the only river that discharges sediment directly into the main body of the Bay; sediment carried by the other major tributaries is largely entrapped within the sub-estuaries (Schubel and Carter, 1976). Fluvial sediment is divided into three classes (clay, silt and sand), each represented with a particular grain size (0.004, 0.008 and 0.069 mm, respectively). The sediment content is 40% clay, 50% silt and 10% sand (Gross et al., 1978). The settling velocities for the three classes of sediment are 0.02, 0.03 and 1.0 mm/s, respectively; the critical erosion shear stresses are 0.013, 0.022 and 0.09 Pa, respectively, corresponding to the grain size (Gelfenbaum and Smith, 1986). Warner et al. (2008) provide the details of the ROMS sediment module, in which the erosion flux is parameterized as

$$E = E_0(1 - \varphi) \frac{\tau_b - \tau_{ce}}{\tau_{ce}}, \quad (1)$$

where  $E$  is the surface erosion mass flux ( $\text{kg}/\text{m}^2/\text{s}^1$ ),  $E_0$  is a bed erodibility constant ( $\text{kg}/\text{m}^2/\text{s}^1$ ),  $\varphi$  is the porosity (volume of voids/total volume) of the top bed layer,  $\tau_{ce}$  is the critical shear stress for erosion, and  $\tau_b$  is the bed shear stress determined by the hydrodynamic routines. The erosion constant is spatially uniform and is chosen to be  $4 \times 10^{-5} \text{ kg}/\text{m}^2/\text{s}$ , following a modeling study of the estuarine turbidity maximum in Chesapeake Bay by North et al. (2004). Because this study mainly concentrates on fluvial sediment, the seabed is simplified and initialized with uniformly distributed silt that has a single grain size of 0.022 mm (North et al., 2004). The resuspension of bottom sediment, with the same erosion constant and a critical shear stress of 0.049 Pa (North et al., 2004), acts as the background for suspended sediment in the Bay. At high suspended-sediment concentrations, the contribution of suspended sediment to water density is included by treating the water as a water–sediment mixture. Because the model runs were intended primarily to investigate the transport and deposition of fluvial sediments during TS Lee, surface waves and their effects were not included. Thus, only the model results for TS Lee are reported here.

As discussed in detail by Cheng et al. (2013), the numerical simulation of the sediment plume is sensitive to sediment parameters. To find appropriate settling velocities for the flood-delivered sediment, we carried out a series of sensitivity-analysis experiments and selected the settling velocities that gave the best prediction for the observed along-estuary distribution of suspended sediment concentration. The numerical model assumed constant settling velocities for each sediment class and neglected effects of flocculation that could be important during large floods (Hill et al., 2000). The observed settling velocity of sediment flocs ranges from 0.3 to 3 mm/s in the ETM region of Chesapeake Bay (Sanford and Maa, 2001). One approach to model the effects of flocculation would be to use an empirical formula of the flocs' settling velocity that varies with the suspended sediment concentration and turbulence dissipation rate or shear-stress magnitude (Burban et al., 1990; Partheniades, 1992). However, such a formula cannot easily be incorporated into ROMS because the calculation of sediment settling is based on a semi-Lagrangian method. Another important sediment parameter is the critical shear stress for each grain size. We chose their values by following a non-dimensional Shields curve that assumes non-cohesive well-sorted particles (Gelfenbaum and Smith, 1986). We conducted a sensitivity experiment in which the critical shear stress of each

grain size is doubled and found a similar deposition pattern of the flood sediment because deposition overwhelmed erosion during the flood period.

Measurements of suspended sediment concentration at the Susquehanna River are required to obtain accurate estimates of sediment loading but no data were collected during TS Lee. To estimate the sediment discharge from the Susquehanna River, we built a regression relation between SSC ( $\text{mg}/\text{l}$ ) and river discharge ( $R$ ,  $\text{m}^3/\text{s}$ ) at Conowingo, Maryland, using an extended set of USGS observational data collected between January 1978 and July 2011 (Michael Langland, personal communication) that include discharge ( $R$ ) up to  $18 \times 10^3 \text{ m}^3/\text{s}^{-1}$ :

$$\text{SSC} = 21.774 \times \exp(2.2286 \times 10^{-4} \times R) - 15.3107 \quad (2)$$

with this formula, a total of  $6.6 \times 10^6 \text{ t}$  of sediment were discharged to Chesapeake Bay between 7 and 17 September 2011. The regression coefficient  $r^2$  is 0.79. With this formula, a total of 6.7 million tons of sediment were discharged to Chesapeake Bay between 7 and 17 September. A loading of 5 million tons was obtained using the formula by Gross et al. (1978) but we decided to use the former since it is based on recent observations. Eq. (2) provides a reasonable estimate of sediment loading during TS Lee, since the model-predicted suspended sediment concentration is in good agreement with the post-storm observations (Cheng et al., 2013). Moreover, the model-predicted total sediment loading during the flood is close to the total deposited mass estimated from sediment core measurements (see Section 3.2 for more details).

### 3. Results

#### 3.1. Physical response of Chesapeake Bay to Hurricane Irene and TS Lee

The physical response of the Bay to the very different storm forcing during TS Lee and Hurricane Irene is illustrated in Fig. 3, which presents representative time series of forcing and response assembled from different monitoring systems. Winds at Thomas Pt Light were as high as 25 m/s directly down the axis of the Bay for several hours during the night of 27 Aug 2011 as Irene passed by. Winds during TS Lee, on the other hand, were indistinguishable from non-storm conditions. As stated above, Susquehanna River flow after Irene was elevated, but dwarfed by flow during and after TS Lee. Susquehanna River sediment loads during TS Lee, estimated using Eq. (2), completely dominated the entire period (and indeed the year). Estimated sediment load peaked at about 5.5 t/day on 9 September 2011, corresponding to an estimated suspended-sediment concentration (SSC) of almost 3 g/l. Surface wave heights measured at the Gooses Reef CBIBS buoy in mid-Bay were up to 3 m during Irene, but only about 0.5 m during TS Lee. Surface wave periods were up to 6 s during Irene, but about 2.5 s during TS Lee. Wave conditions during Irene seem extreme in such a fetch-limited environment (Lin et al., 2002), but were verified by comparison to independent observations collected several kilometers to the south (Malcolm Scully, personal communication). Waves measured at CBIBS buoys further up the Bay were progressively smaller and of shorter periods, consistent with fetch limitation. Surface turbidity measured at Gooses Reef spiked sharply during Irene, in phase with the highest wave forcing. After TS Lee, surface turbidity at Gooses Reef lagged behind the peak in Susquehanna River loads by almost 4 days, but was approximately twice as high as during Irene and remained elevated for several days, corresponding to the plume of Fig. 1 passing the Gooses Reef site. No local data on SSC were available to convert turbidity to SSC at Gooses Reef.

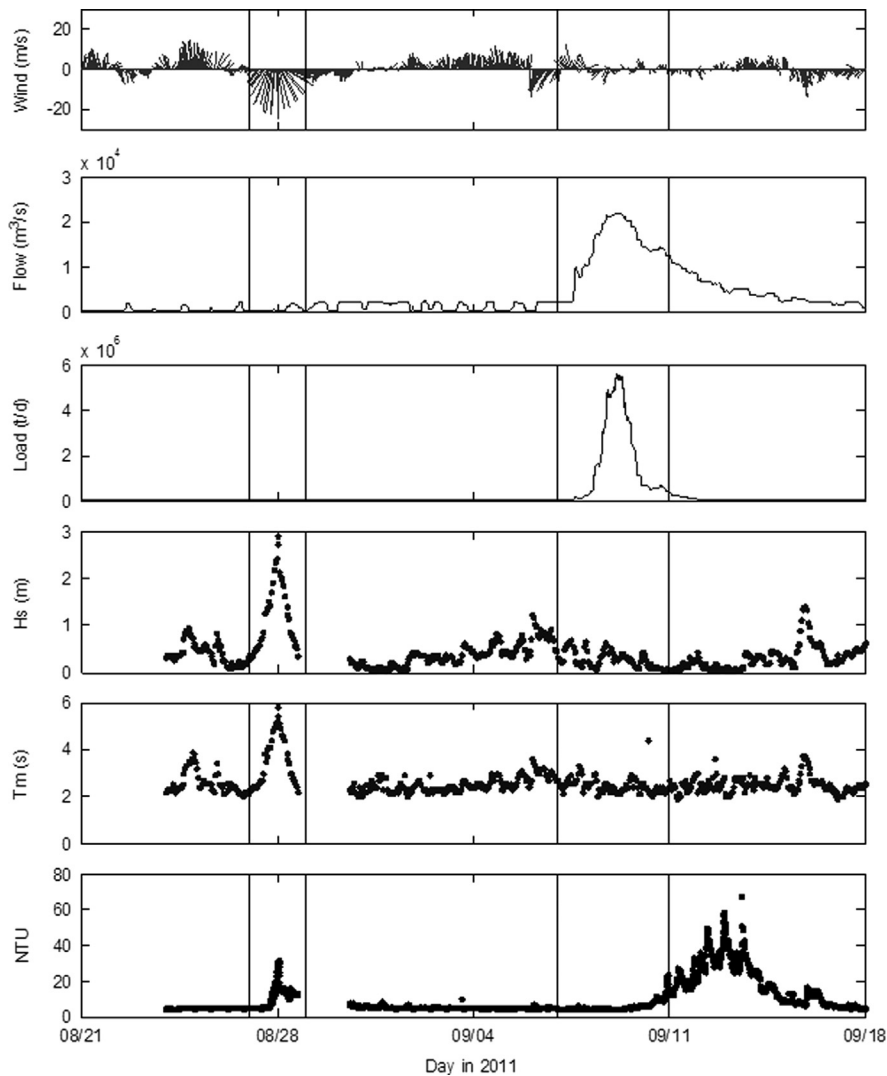


**Fig. 3.** Time series of selected environmental forcings and Chesapeake Bay responses during late August and early September, 2001. Top panel—Wind vectors from Thomas Pt. Light, with vectors pointing in the direction towards which the wind was blowing. Second panel—Susquehanna River flow at Conowingo Dam measured at 15-min intervals. The small scale, short-term pulsed signature under low flows represents flow control by the hydro-electric power plant. Third panel—Suspended-sediment load at Conowingo Dam, estimated as cited in text. Fourth panel—Significant wave height measured at the Gooses Reef buoy. Fifth panel—Mean wave period measured at Gooses Reef buoy. Bottom panel—Near-surface turbidity measured at Gooses Reef buoy. Vertical lines in all panels enclose the approximate periods of Hurricane Irene and Tropical Storm Lee.

### 3.2. Sedimentological characteristics of the flood deposit and estimated deposit mass

The flood deposit was identified in cores by its relatively fine grain size, uniform  $^7\text{Be}$  activities, and physical stratification in x-radiographs. Sediments deposited in the central deeper portions of the upper Chesapeake Bay generally consist of fine grained muds transitioning from predominantly clayey silts north of Lee3 to silty clays to the south (Kerhin et al., 1988). The flood deposit could not be identified in x-radiographs by a coarsening in grain size as has been recognized in storm deposits on open coastal areas with large fetch and significant wave action (Bentley et al., 2002; Keen et al., 2006). Rather the flood deposit was identified in the x-radiographs as a more transparent layer indicative of higher water content and rapid deposition, or by burial of benthic epifauna. Bioturbation has not been observed to significantly disrupt primary sedimentary features in the oligohaline portion of the Chesapeake Bay (Reinharz et al., 1982; Maryland Geological Survey, unpublished data). The flood deposit commonly had a relatively fine grain size and uniform  $^7\text{Be}$  activities. Surficial sediments were muddy, with median diameters ranging from 1.4

to 18.6  $\mu\text{m}$ , with most values between 2 and 6  $\mu\text{m}$  (Table 1). Grain size within the top 6 cm of each core was relatively uniform, with some downward coarsening like that observed at Lee7 (Fig. 4a).  $^7\text{Be}$  penetration depths ranged from 0 cm (not detectable) to 4 cm; these depths were greatest in the northern Bay, decreasing southward.  $^7\text{Be}$  was not detected north of Lee7 or south of LeeS2. Flood-deposit thicknesses derived from the x-radiographs generally agreed with the maximum penetration depth of  $^7\text{Be}$ , although the  $^7\text{Be}$  depths were often 1 cm greater (Table 1). The largest discrepancy occurred at LeeS3, where  $^7\text{Be}$  was not detected but a thick ( $\sim 10$  cm) unit of physically stratified sediments was observed in the x-radiograph (Fig. 4b).

Using the maximum penetration depth of  $^7\text{Be}$  as proxy for flood-deposit thickness, a map of the flood deposit was produced using ArcGIS using a kriging interpolation, which is commonly utilized to analyze irregularly spaced data (Fig. 5). This map showed an apparent depocenter at Lee6 and Lee7, south of which deposition decreased rapidly, resulting in a thin drape of flood sediment in most of the upper Chesapeake Bay. Little to no flood sediment was likely deposited south of LeeS2. A deposit mass can be estimated using this map by assuming a sediment bulk density.

Recently deposited sediments in northern Chesapeake Bay have a water content of  $\sim 60\%$  (Sanford and Halka, 1993; Maryland Geological Survey, unpublished data), which translates to a dry bulk density of  $0.5 \text{ g/cm}^3$ , assuming a grain density of  $2.65 \text{ g/cm}^3$ . The resulting calculated deposit mass is  $4.9 \times 10^6 \text{ t}$ , which represents  $\sim 70\%$  of the estimated  $6.7 \times 10^6 \text{ t}$  of sediment delivered by the remnants of Tropical Storm Lee (Cheng et al., 2013). Note that recently delivered flood sediment may have higher water content;

this would result in a lower dry bulk density value and hence a lower deposit-mass estimate.

### 3.3. Wave-induced bottom stresses during Irene

Estimated wave-induced bottom stresses at the latitude of LeeS3 at the peak of Hurricane Irene were as high as  $7 \text{ Pa}$  (Fig. 6), much higher than typical tidal bottom stresses ( $\sim 0.2 \text{ Pa}$ ; Sanford and Halka, 1993; Wright et al., 1992) and higher than mid-Bay maximum current generated stresses during Irene as modeled without waves ( $0.5\text{--}2 \text{ Pa}$ ). In depths less than  $7 \text{ m}$ , wave orbital velocities were greater than  $1 \text{ m/s}$  and wave stresses were greater than  $3 \text{ Pa}$ , more than an order of magnitude higher than the critical stress for significant erosion. At the depth of core S3 (about  $15 \text{ m}$ ), estimated orbital velocities were  $> 0.35 \text{ m/s}$  and wave-induced bottom stresses were about  $0.6 \text{ Pa}$ , still significantly higher than the estimated critical stresses for erosion. Even at the thalweg depth of  $26 \text{ m}$ , wave-induced bottom stresses equaled the critical stress for initial erosion. Clearly, these stresses were sufficient to cause significant erosion of bottom sediments, with a strong gradient from extreme erosion in shallow waters to low erosion or deposition in the deepest waters. Total stresses were likely even higher because of simultaneous wind-enhanced currents, especially in the deep channel. It is well-known that non-linear interactions between waves and currents in the bottom boundary layer can lead to enhanced total stresses (Grant and Madsen, 1979). Quantitative estimation of wave-current stresses and entrainment dynamics is beyond the scope of this study, however; we seek only to demonstrate that extreme erosion was

**Table 1**  
Flood-deposit thicknesses derived from  $^7\text{Be}$  penetrations depths and x-radiographs, as well as the median diameter of surficial (top  $1 \text{ cm}$ ) sediments. Stations are listed from north to south.

Station	$^7\text{Be}$ depth (cm)	X-radiograph depth (cm)	Median diameter (top $1 \text{ cm}$ ; $\mu\text{m}$ )
Lee8	0	0	18.6
Lee7	4	2–3 or 7	3.9
Lee6.5	2	0	3.6
Lee6	4	3	2.3
Lee5	2	1	4.4
Lee4	1	0–2	5.6
Lee3	0	0–1	5.1
Lee2.5	1	1	3.5
Lee2	1	1	2.2
Lee1	1	1–2	2.4
Lee0.5	0	0	4.8
Lee0	1	0	1.4
LeeS1	1	1–2	2.9
LeeS2	1	0	3.9
LeeS3	0	10	3.6
LeeS4	0	0 or 2	8.1

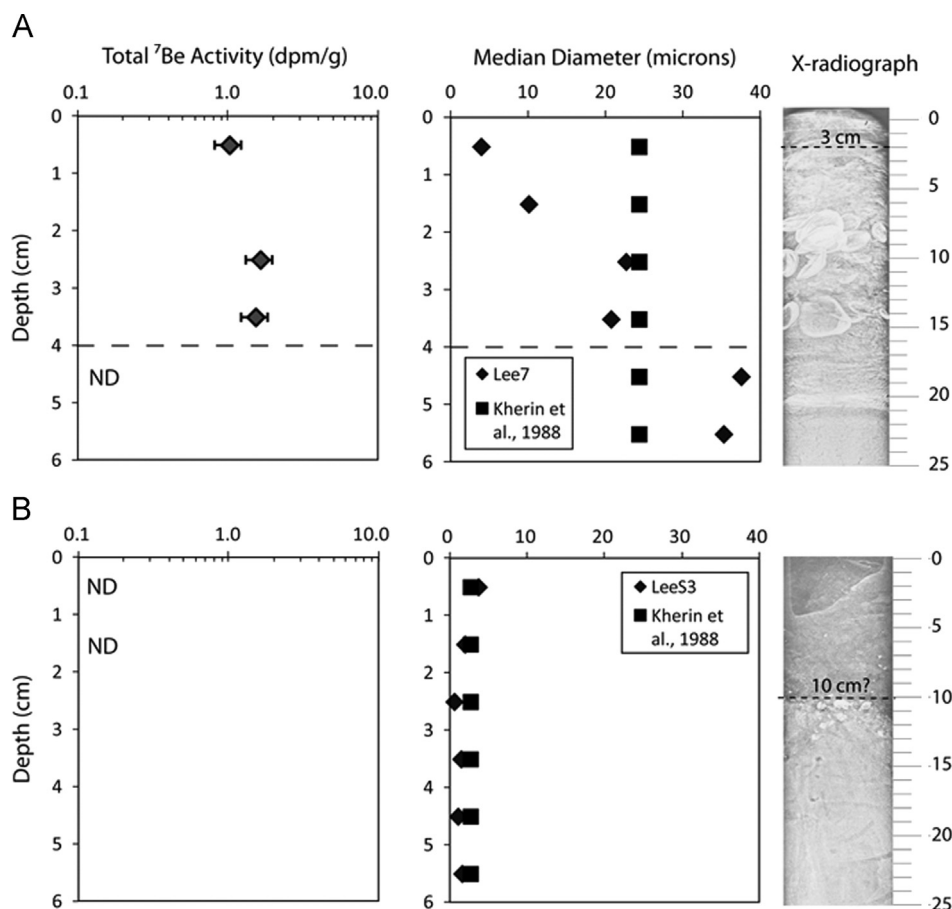


**Fig. 4.** (Left to right) Profiles of  $^7\text{Be}$ , grain size (median diameter), and x-radiographs for the upper  $6 \text{ cm}$  of (A) Lee7 and (B) LeeS3. Dotted lines indicate the interpreted depth of flood-deposit thickness in the x-radiographs. ND=not detected.

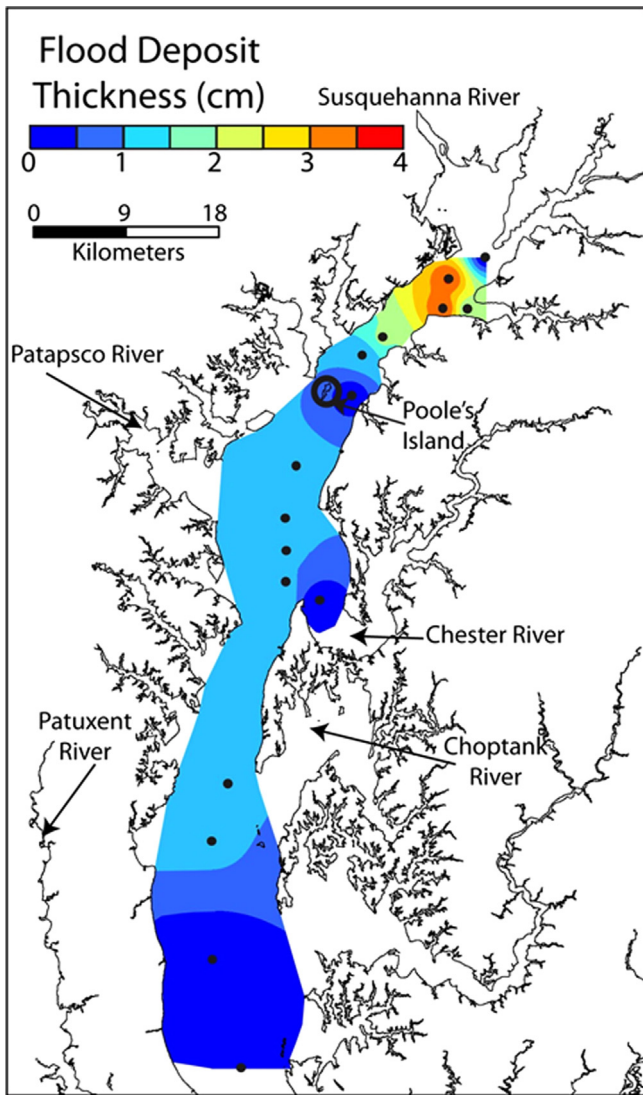


Fig. 5. Spatial interpolation of <sup>7</sup>Be maximum penetration depths over the study area, performed in ArcGIS.

likely during Hurricane Irene. Vertical mixing of the water column during strong wind events (Goodrich et al., 1987; Li et al., 2007), combined with dispersion of the eroded sediments above the wave boundary layer by current-induced mixing (Sanford, 1994) likely distributed at least some of this sediment throughout the water column and led to the peak in surface turbidity observed at Gooses Reef, which coincided with the peak in wave forcing. Approximately 30% of the cross-section was likely impacted by depth-limited breaking, corresponding closely to the regions identified as sandy in a previous comprehensive bottom sediment mapping effort for northern Chesapeake Bay (Kerhin et al., 1988).

3.4. Sediment transport model results for TS Lee

The coupled hydrodynamic-sediment-transport model tracks sediment transport by estuarine circulation, deposition due to settling, and resuspension due to tidal stress. As shown in Fig. 7, high surface suspended-sediment concentrations (SSC) reached from the Susquehanna River to the mouth of the Potomac River on September 13, covering about half of Chesapeake Bay. This massive brown sediment plume was also captured in satellite images (see Fig. 1b). Cheng et al. (2013) show that the delivery of fluvial sediment to the Chesapeake Bay underwent 3 stages during the

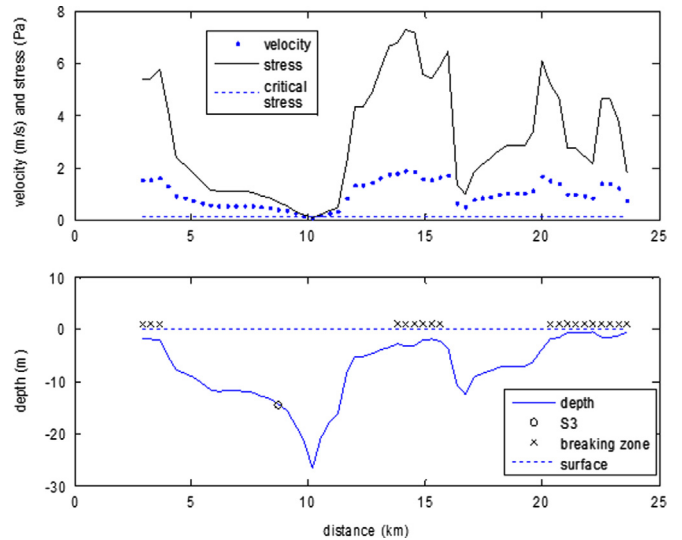


Fig. 6. Estimated wave effects on the bottom across a lateral transect at the latitude of LeeS3 at the peak of Hurricane Irene on 28 August 2011. Estimates based on a 2.5 m high, 5.5 s period surface wave. Top panel—Maximum bottom stress, maximum bottom velocity, and estimated critical stress for initial sediment erosion. Bottom panel—Depth, likely zones of depth-limited breaking, and location of LeeS3.

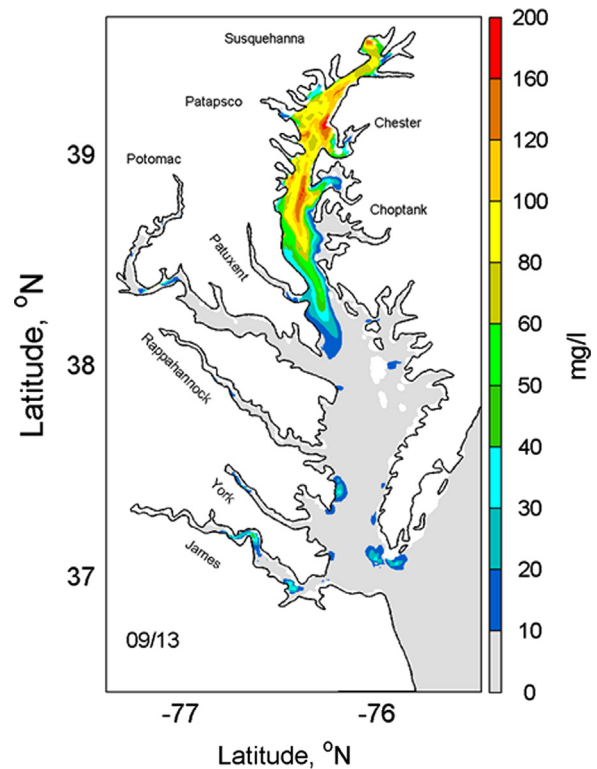


Fig. 7. Distribution of model-predicted surface suspended sediment concentration on 13 September 2011.

passage of TS Lee. During the first stage, between 7 and 10 September, flood waters forced the salt front downstream by 30 km and loaded the shallow upper Bay with SSC exceeding 2500 mg/l. During the second stage, between 10 and 18 September, the strong horizontal salinity gradient set up by TS Lee produced two-layer flows with speeds reaching 0.3 m/s, and the strong seaward surface currents rapidly transported sediment downstream. This current is 2–3 times larger than the typical residual current in Chesapeake Bay (Li et al., 2005). In the third

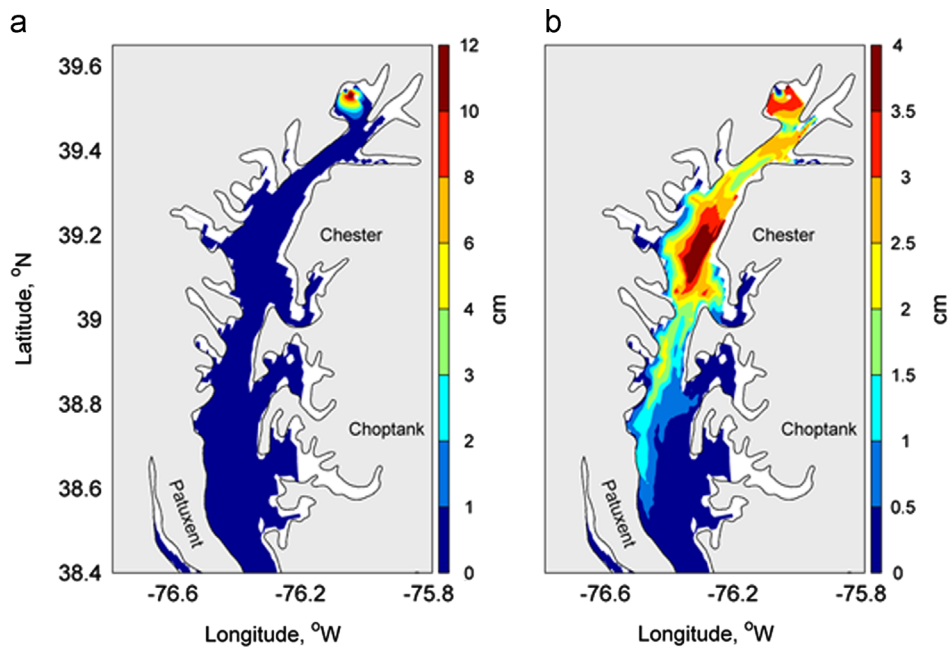


Fig. 8. Model-predicted thickness of fluvial sediment deposits on 28 September 2011: (a) sands, (b) clays and silts. The units are in cm.

stage, between 18 and 25 September, settling became the dominant process. Large amounts of fluvial sediment settled to the seabed, while the rest of the sediments in the surface layer were advected further seaward.

Fig. 8 shows the spatial distribution of the modeled deposited fluvial sediment on 28 September 2011, when the first field cruise was conducted (we also plotted the sediment deposition on 24 October 2011 and found very similar distributions). Most of the sands were deposited on the Susquehanna Flats, where the maximum thickness of new sediment was nearly 10 cm (Fig. 8a). A thinner deposit of fine-grained fluvial sediment (clay and silt) was predicted in the other part of the upper Bay, exhibiting clear cross-estuary variability (Fig. 8b). Most fine-grained sediment in the upper Bay accumulated near the eastern shore, with a maximum thickness of 3.5 cm above the mouth of the Chester River. Further downstream in the wider mid-Bay region, the sediment plume was confined to the western shore due to the Coriolis force so that the deposition of fine-grained sediment was constricted near the western shore, with a thickness of 1.5 cm. The deposition time of the fine-grained sediment depends on its settling velocity. For a typical water depth of 20 m in the mid- and upper Bay, it takes nearly 12 days for the clay component to settle on the bed. This is consistent with the accumulation time of the fine-grained sediment on the bottom of the Bay. The settling velocity of the sand component is much larger (1 mm/s), allowing the sand to settle through a 20-m water column in less than 6 h. Therefore, the sand component of the fluvial sediment was mainly deposited near the mouth of the Susquehanna River. Based upon the model simulation, we estimated that approximately 18 days after the flood (28 September 2011), nearly  $6.73 \times 10^6$  t of fluvial sediment deposited inside the Bay,  $0.15 \times 10^6$  t remained in the water column, and only 307 t of fluvial sediment escaped from the Bay, accounting for less than 0.01% of the total sediment carried by the flood.

#### 4. Discussion

The thickness and extent of flood-sediment deposition have been documented adjacent to many fluvial systems around the

world (e.g., adjacent to the Po, Eel, and Mississippi Rivers), using signatures of  $^7\text{Be}$  and x-radiographs observed from sediment cores (Dail et al., 2007; Palinkas et al., 2005; Wheatcroft et al., 2006). These signatures tend to agree in fluvial systems with relatively small watersheds, where sediment can be rapidly eroded from the watershed and delivered to the adjacent aquatic environment without prolonged storage, limiting  $^7\text{Be}$  decay (e.g., the Eel River case; Sommerfield et al., 1999). However, these signatures tend to disagree in fluvial systems with larger watersheds, where the first sediment deposited during floods is older riverbed sediment that lacks detectable  $^7\text{Be}$  but is physically stratified in x-radiographs (e.g., the Po River case; Palinkas et al., 2005; Wheatcroft et al., 2006). Susquehanna River sediments deposited after TS Lee could be expected to have characteristics of both cases—extremely high river discharge is energetic enough to keep newly eroded sediments in suspension until they reached the upper Bay, but sediments stored behind Conowingo Dam are sequestered until river discharge reaches the scour threshold during infrequent large events. In the 10 years preceding the passage of TS Lee, the scour threshold for the Conowingo was only exceeded on three occasions: 19 and 20 September 2004 (daily mean discharges at Conowingo of 14,017 and 15,433  $\text{m}^3/\text{s}$ , respectively), 29 June 2006 (11,412  $\text{m}^3/\text{s}$ ), 12 March 2011 (11,752  $\text{m}^3/\text{s}$ ). Thus, using  $^7\text{Be}$  maximum penetration depths to determine the flood deposit thickness in upper Chesapeake Bay could result in an underestimate. However,  $^7\text{Be}$  penetration depths in this study tend to agree or be  $\sim 1$  cm greater than x-radiographs (except at LeeS3, discussed below). This discrepancy could arise from the 1-cm sampling increments used in the  $^7\text{Be}$  measurements and the difficulty of recognizing thin horizons in x-radiographs. For example, at Lee7 (see Fig. 4a), the  $^7\text{Be}$  penetration depth was 4 cm but only 2–3 cm of flood sediment was recognized in the x-radiograph. Small amounts of flood sediment could be present in the 3–4-cm interval of the core, such that  $^7\text{Be}$  activities are high enough to be detected but correspond to only a few millimeters of deposition (e.g., 3.1 cm of flood deposition would be recorded as 4 cm). Similarly, in the x-radiograph, the horizon is estimated to the nearest centimeter, and a 3.1-cm deposit could be recorded as 3 cm. The general agreement of  $^7\text{Be}$  and x-radiograph estimates of flood deposition implies that sediment originating from behind Conowingo

Dam, which should not have detectable  $^7\text{Be}$ , is “missing” from the core samples. This sediment could be mixed with the newly eroded ( $^7\text{Be}$ -tagged) sediment from the watershed such that  $^7\text{Be}$  activities are diluted but still detectable. Or, Conowingo sediment could simply not be present at our specific core locations. Since the deposition pattern observed following TS Lee is similar to that observed following TS Agnes in 1972, although thinner due to lower sediment delivery during TS Lee, the former scenario is most likely.

The largest discrepancy between  $^7\text{Be}$  and x-radiograph observations is at LeeS3 (see Fig. 4b), where  $^7\text{Be}$  is not present but physical stratification is observed in the top 10 cm of the core. This discrepancy can be explained by erosion, transport, and redeposition of sediments during Hurricane Irene, creating physical stratification that is not associated with TS Lee-related flood-sediment deposition. Similar centimeters-thick storm-generated mud deposits have been identified in several continental shelf locations, including the Atchafalaya shelf in the Gulf of Mexico (Jaramillo et al., 2009), the Northern California shelf off the Eel River (Traykovski et al., 2000), and the Po River delta in the Adriatic Sea (Friedrichs and Scully, 2007). In all of these cases, wave-forced fluid muds were implicated in formation of the storm deposits. Fluid-mud layers supported by wave forcing also have been shown to transport large amounts of sediment downslope and offshore (Friedrichs and Scully, 2007; Traykovski et al., 2000), leading to accumulation where the wave energy is no longer competent to support suspension. Although it is not clear whether fluid muds were involved in the present case, it is likely that the 10-cm thick storm layer observed at LeeS3 represents accumulation of muds transported offshore during or after the storm. Storm wave-generated offshore transport is consistent with the fact that nearshore sediments in the mid-Bay are predominantly sandy with low rates of accumulation or even erosion, while deep channel sediments are predominantly muddy and experience high rates of deposition, even though the dominant source of these sediments is shoreline erosion in the mid-Bay (Hobbs et al., 1992). Wave forcing during Irene was significantly weaker further north in the Bay, so deep-water sediments might not have been affected as much.

Note that both  $^7\text{Be}$  and x-radiograph techniques could include sedimentation from Hurricane Irene and/or a pulse in Susquehanna discharge that occurred in late September 2011, although this late-September discharge only reached  $5663 \text{ m}^3/\text{s}$ , approximately half the discharge needed for significant scour. However, model runs can isolate specific events and can track very thin sediment deposits at much higher spatial resolution. In general, there is agreement on the deposition thickness between the  $^7\text{Be}$  and model estimates, as shown in the comparison between Figs. 5 and 8. The best agreement occurs in the northern portion of the study area, near the Susquehanna River, where both show a relatively thick depocenter (2.5–3 cm in the model; 4-cm  $^7\text{Be}$  penetration depth). They also agree in the southern portion of the study area, with both suggesting little to no sediment deposited south of the Choptank River. This lends further support to our interpretation of the physical stratification observed in core LeeS3 and described above. The largest discrepancy occurs near Poole's Island, where the model predicts ~3 cm of deposition but no  $^7\text{Be}$  was detected. This may be due to a combination of shallow water depths, a constricted channel, and strong wave forcing following TS Lee. Fig. 3 shows that a reasonably strong wind-wave event occurred on 16 September 2011, after TS Lee but before the first coring cruise. Sanford (1994) showed that even moderate wind events can generate large wave-forced sediment resuspension near Poole's Island, and the recent storm deposits would have been unconsolidated and easy to erode. The present model might not have predicted as much resuspension at this location because it did not include wave forcing.

The field and model observations yield similar deposit geometry and mass. This is somewhat unexpected, given that the field-based deposit mass is a rough, order-of-magnitude estimate for several reasons. First, the areas used in the calculation extend to the shoreline in most cases and all boundaries were somewhat arbitrary, chosen to exclude potential transport into tributaries. Also, no sediment was assumed to deposit from LeeS3 southward, based on the absence of  $^7\text{Be}$  or any other clear flood-sediment signatures. In reality, it is unlikely that flood sediment was deposited in shallow (less than a few meters or so) areas and some sediment may have entered tributaries. It is also likely that some sediment was transported southward but cannot be resolved using our analysis techniques. Finally, the 1-cm sampling increments would overestimate a “dusting” of sediment (i.e., a few millimeters would be included as 1 cm), as previously mentioned.

In this study, the combination of field observations and model simulations has yielded improved understanding of sediment dynamics during storm events. While the potential lasting effects of TS Lee-related sedimentation are not yet clear, a review of SAV response to sediment burial suggests that 50% mortality can occur with as little as 2 cm burial (Cabaco et al., 2008). It would be tempting to conclude that these types of large sedimentation events, while detrimental to the Bay's ecosystem, are infrequent (i.e., 40 years lapsed between TS Agnes and TS Lee). However, the US East and Gulf coasts have experienced elevated tropical storm and hurricane activity in recent years, and this pattern is expected to continue or even accelerate in the future due to global warming (Emanuel, 2005; Goldenberg et al., 2001; Webster et al., 2005). It is thus critical to understand the sediment transport and deposition that likely results from these events, especially as it ultimately controls the fate of particle-attached nutrients and pollutants.

## 5. Summary

This study used  $^7\text{Be}$  and x-radiographs to identify flood deposition associated with TS Lee in sediment cores. These results were compared to model simulations of sediment dynamics during the event. Both field and model results indicated that the thickest sediment deposits were located near the Susquehanna River mouth, and these deposits were ~4 cm thick. However, the sediment accumulated in this area did not account for the full mass of sediment delivered. Instead, much of the sediment was transported southward and deposited as a relatively thin but widespread layer of new material. This widespread deposition was also strongly suggested by the southward extent of the turbidity plume observed in the satellite image, although this image only represents surface suspended sediment. There was one exception of a sediment core with physical stratification but no  $^7\text{Be}$  activity. This discrepancy can be explained by extreme wave activity during Hurricane Irene that eroded, transported, and redeposited sediments in the southern portion of the Bay. Thus study highlights the improved understanding of flood-sediment transport and fate that can be gained by integrating field observations and model simulations.

## Acknowledgements

The authors would like to thank the captain and mate of the R/V *Kherin*, Rick Younger and Keith Lindemann, who assisted in both coring cruises. Thanks are also due to Steve VanRyswick of the Maryland Geological Survey who assisted in collecting the cores and conducted all the x-ray work. Funding for the Maryland Geological Survey and vessel time was provided by the Environmental Protection Agency grant CB-97354505. Sanford, Li, and

Cheng received funding from the National Science Foundation grants OCE-1061609 and OCE-082543, Palinkas received funding from the Grayce B. Kerr Fund grant 07-55014. This is UMCES contribution number 4760.

## References

- Allison, M.A., Kineke, G.C., Gordon, E.S., Goni, M.A., 2000. Development and reworking of a seasonal flood deposit on the inner continental shelf off the Atchafalaya River. *Continental Shelf Research* 20, 2267–2294.
- Baskaran, M., Santschi, P.H., 1993. The role of particles and colloids in the transport of radionuclides in coastal environments of Texas. *Marine Chemistry* 43, 95–114.
- Bentley, S.J., Keen, T.R., Blain, C.A., Vaughan, W.C., 2002. The origin and preservation of a major hurricane event bed in the northern Gulf of Mexico: Hurricane Camille, 1969. *Marine Geology* 186, 423–446.
- Bentley, S.J., Sheremet, A., Jaeger, J.M., 2006. Event sedimentation, bioturbation, and preserved sedimentary fabric: field and model comparisons in three contrasting marine settings. *Continental Shelf Research* 26, 2108–2124.
- Bever, A.J., Harris, C.K., Sherwood, C.R., Signell, R.P., 2009. Deposition and flux of sediment from the Po River, Italy: An idealized and wintertime numerical modeling study. *Marine Geology* 260, 69–80.
- Burban, P.Y., Xu, Y., McNeil, J., Lick, W., 1990. Settling speeds of flocs in fresh and sea waters. *Journal of Geophysical Research* 95 (C10), 18213–18220.
- Cabaco, S., Santos, R., Duarte, C.M., 2008. The impact of sediment burial and erosion on seagrasses: a review. *Estuarine Coastal and Shelf Science* 79, 354–366.
- Cheng, P., Li, M., Li, Y., 2013. Generation of an estuarine sediment plume by a tropical storm. *Journal of Geophysical Research* 118, 856–868, <http://dx.doi.org/10.1002/jgrc.20070>. (2013).
- Dail, M.B., Reide Corbett, D., Walsh, J.P., 2007. Assessing the importance of tropical cyclones on continental margin sedimentation in the Mississippi delta region. *Continental Shelf Research* 27, 1857–1874.
- Dickey, T.D., Chang, G.C., Agrawal, Y.C., Williams, A.J., Hill, P.S., 1998. Sediment resuspension in the wakes of hurricanes Edouard and Hortense. *Geophysical Research Letters* 25, 3533–3536.
- Emanuel, K., 2005. Increasing destructiveness of tropical cyclones over the past 30 years. *Nature* 436, 686–688.
- Friedrichs, C.T., Scully, M.E., 2007. Modeling deposition by wave-supported gravity flows on the Po River prodelta: from seasonal floods to prograding clinoforms. *Continental Shelf Research* 27, 322–337.
- Gallucci, F., Netto, S.A., 2004. Effects of the passage of cold fronts over a coastal site: an ecosystem approach. *Marine Ecology-Progress Series* 281, 79–92.
- Gelfenbaum, G., Smith, J.D., 1986. Experimental evaluation of a generalized suspended-sediment transport theory. In: Knight, R.J., McClean, J.R. (Eds.), *Sand and Sandstones, Memoir II*. Canadian Society of Petroleum Geologists, Calgary, pp. 133–144.
- Goldenberg, S.B., Landsea, C.W., Mestas-Nunez, A.M., Gray, W.M., 2001. The recent increase in Atlantic hurricane activity: causes and implications. *Science* 293, 474–479.
- Goodrich, D.M., Boicourt, W.C., Hamilton, P., Pritchard, D.W., 1987. Wind-induced destratification in Chesapeake Bay. *Journal of Physical Oceanography* 17, 2232–2240.
- Grant, W.D., Madsen, O.S., 1979. Combined wave and current interaction with a rough bottom. *Journal of Geophysical Research—Oceans and Atmospheres* 84, 1797–1808.
- Gross, M.G., Karweit, M., Cronin, W.B., Schubel, J.R., 1978. Suspended sediment discharge of the Susquehanna River to northern Chesapeake Bay, 1966 to 1976. *Estuaries* 1, 106–110.
- Haidvogel, D.B., Arango, H.G., Hedstrom, K., Beckmann, A., Malanotte-Rizzoli, P., Shchepetkin, A.F., 2000. Model evaluation experiments in the North Atlantic Basin: simulations in nonlinear terrain-following coordinates. *Dynamics of Atmospheres and Oceans* 32, 239–281.
- Hill, P.S., Milligan, T.G., Geyer, W.R., 2000. Controls on effective settling velocity of suspended sediment in the Eel River flood plume. *Continental Shelf Research* 20, 2095–2111.
- Hirsch, R.M., 2012. Flux of Nitrogen, Phosphorus, and Suspended Sediment from the Susquehanna River Basin to the Chesapeake Bay During Tropical Storm Lee, September 2011, as an Indicator of the Effects of Reservoir Sedimentation on Water Quality. US Geological Survey Scientific Investigations Report 2012-5185, 17pp.
- Hobbs, C.H., Halka, J.P., Kerhin, R.T., Carron, M.J., 1992. Chesapeake Bay sediment budget. *Journal of Coastal Research* 8, 292–300.
- Jaramillo, S., Sheremet, A., Allison, M.A., Reed, A.H., Holland, K.T., 2009. Wave-mud interactions over the muddy Atchafalaya subaqueous clinoform, Louisiana, United States: wave-supported sediment transport. *Journal of Geophysical Research—Oceans*, 114.
- Keen, T.R., Furukawa, Y., Bentley, S.J., Slingerland, R.L., Teague, W.J., Dykes, J.D., Rowley, C.D., 2006. Geological and oceanographic perspectives on event bed formation during Hurricane Katrina. *Geophysical Research Letters*, 33.
- Kerhin, R., Halka, J., Wells, D.V., Hennessee, E.L., Blakeslee, P.J., Zoltan, N., Cuthbertson, R.H., 1988. The surficial sediments of Chesapeake Bay, Maryland: physical characteristics and sediment budget. Maryland Geological Survey, Baltimore p. 43.
- Kerwin, J.A., Munro, R.E., Peterson, W.A., 1976. Distribution and abundance of aquatic vegetation in the upper Chesapeake Bay, 1971–1974. In: Ruzecki, E.P., et al. (Eds.), *The Effects of Tropical Storm Agnes on the Chesapeake Estuarine System*. CRC Publication 54. The Johns Hopkins University Press, Baltimore and London, pp. 393–400.
- Langland, M., Cronin, T., 2003. A Summary Report of Sediment Processes in Chesapeake Bay and Watershed. US Geological Survey Water-Resources Investigations Report 03-4123, 109 pp.
- Larsen, I.L., Cutshall, N.H., 1981. Direct determination of  $^{7}\text{Be}$  in sediments. *Earth and Planetary Science Letters* 54, 379–384.
- Li, M., Zhong, L.J., Boicourt, W.C., 2005. Simulations of Chesapeake Bay estuary: sensitivity to turbulence mixing parameterizations and comparison with observations. *Journal of Geophysical Research—Oceans* 110, C12004, <http://dx.doi.org/10.1029/2004JC002585>.
- Li, M., Zhong, L.J., Boicourt, W.C., Zhang, S.L., Zhang, D.L., 2006. Hurricane-induced storm surges, currents and destratification in a semi-enclosed bay. *Geophysical Research Letters* 33, L02604, <http://dx.doi.org/10.1029/2005GL024992>.
- Li, M., Zhong, L.J., Boicourt, W.C., Zhang, S.L., Zhang, D.L., 2007. Hurricane-induced destratification and restratification in a partially-mixed estuary. *Journal of Marine Research* 65, 169–192.
- Lin, W.Q., Sanford, L.P., Suttles, S.E., 2002. Wave measurement and modeling in Chesapeake Bay. *Continental Shelf Research* 22, 2673–2686.
- Loftus, M.E., Seliger, H.H., 1976. A comparative study of primary production and standing crops of phytoplankton in a portion of the upper Chesapeake Bay subsequent to Tropical Storm Agnes. In: Ruzecki, E.P., et al. (Eds.), *The Effects of Tropical Storm Agnes on the Chesapeake Estuarine System*. CRC Publication 54. The Johns Hopkins University Press, Baltimore and London, pp. 509–521.
- Madsen, O.S., 1976. Wave climate of the continental margin: elements of its mathematical description. In: Stanley, D.J., Swift, D.J.P. (Eds.), *Marine Sediment Transport and Environmental Management*. John Wiley & Sons, New York, pp. 65–87.
- Nichols, M.M., 1977. Response and recovery of an estuary following a river flood. *Journal of Sedimentary Petrology* 47, 1171–1186.
- North, E.W., Chao, S.Y., Sanford, L.P., Hood, R.R., 2004. The influence of wind and river pulses on an estuarine turbidity maximum: numerical studies and field observations in Chesapeake Bay. *Estuaries* 27, 132–146.
- Olsen, C.R., Larsen, I.L., Lowry, P.D., Cutshall, N.H., Nichols, M.M., 1986. Geochemistry and deposition of Be-7 in river-estuarine and coastal waters. *Journal of Geophysical Research—Oceans* 91, 896–908.
- Palinkas, C.M., Nittrouer, C.A., Wheatcroft, R.A., Langone, L., 2005. The use of Be-7 to identify event and seasonal sedimentation near the Po River delta, Adriatic Sea. *Marine Geology* 222, 95–112.
- Partheniades, E., 1992. Estuarine sediment dynamics and shoaling processes. In: Herbick, J. (Ed.), *Handbook of Coastal and Ocean Engineering*, vol. 3. Gulf Professional Publishing, Houston, Texas, pp. 985–1071.
- Reinharz, E., Nilsen, K.J., Boesch, D.F., Bertelsen, R., O'Connell, A.E., 1982. A Radio-graphic Examination of Physical and Biogenic Sedimentary Structures in the Chesapeake Bay. Maryland Geological Survey, Report of Investigations No. 36, 57 p.
- Sanford, L.P., 1994. Wave-forced resuspension of upper Chesapeake Bay muds. *Estuaries* 17, 148–165.
- Sanford, L.P., 2006. Uncertainties in sediment erodibility estimates due to a lack of standards for experimental protocols and data interpretation. *Integrated Environmental Assessment and Management* 2, 29–34.
- Sanford, L.P., Halka, J.P., 1993. Assessing the paradigm of mutually exclusive erosion and deposition of mud, with examples from upper Chesapeake Bay. *Marine Geology* 114, 37–57.
- Sanford, L.P., Maa, J.P.-Y., 2001. A unified erosion formulation for fine sediments. *Marine Geology* 179, 9–23.
- Schubel, J.R., 1972. Suspended sediment discharge of the Susquehanna River at Conowingo, Maryland, during 1969. *Chesapeake Science* 13, 53–58.
- Schubel, J.R., 1976. Effects of Agnes on the suspended sediment of the Chesapeake Bay and contiguous shelf waters. In: Ruzecki, E.P., et al. (Eds.), *The Effects of Tropical Storm Agnes on the Chesapeake Estuarine System*. CRC Publication 54. The Johns Hopkins University Press, Baltimore and London, pp. 179–200.
- Schubel, J.R., Carter, H.H., 1976. Suspended sediment budget for Chesapeake Bay. In: Wiley, M. (Ed.), *Estuarine Perspectives*, vol. II. Academic Press, New York, pp. 48–62.
- Schubel, J.R., Hirschberg, D.J., 1978. Estuarine graveyards, climatic change, and the importance of the estuarine environment. In: Wiley, M. (Ed.), *Estuarine Interactions*. Academic Press, New York, pp. 285–303.
- Sommerfield, C.K., Nittrouer, C.A., Alexander, C.R., 1999. Be-7 as a tracer of flood sedimentation on the northern California continental margin. *Continental Shelf Research* 19, 335–361.
- Traykovski, P., Geyer, W.R., Irish, J.D., Lynch, J.F., 2000. The role of wave-induced density-driven fluid mud flows for cross-shelf transport on the Eel River continental shelf. *Continental Shelf Research* 20, 2113–2140.
- Warner, J.C., Sherwood, C.R., Signell, R.P., Harris, C.K., Arango, H.G., 2008. Development of a three-dimensional, regional, coupled wave, current, and sediment-transport model. *Computers & Geosciences* 34, 1284–1306.
- Webster, P.J., Holland, G.J., Curry, J.A., Chang, H.R., 2005. Changes in tropical cyclone number, duration, and intensity in a warming environment. *Science* 309, 1844–1846.
- Wheatcroft, R.A., Drake, D.E., 2003. Post-depositional alteration and preservation of sedimentary event layers on continental margins. I. The role of episodic sedimentation. *Marine Geology* 199, 123–137.

- Wheatcroft, R.A., Stevens, A.W., Hunt, L.M., Milligan, T.G., 2006. The large-scale distribution and internal geometry of the fall 2000 Po River flood deposit: evidence from digital x-radiography. *Continental Shelf Research* 26, 499–516.
- Wright, L.D., Boon, J.D., Xu, J.P., Kim, S.C., 1992. The bottom boundary layer of the Bay Stem Plains environment of the lower Chesapeake Bay. *Estuarine Coastal and Shelf Science* 35, 17–36.
- Yarbro, L.A., Carlson, P.R., Fisher, T.R., Chanton, J.P., Kemp, W.M., 1983. A sediment budget for the Choptank River Estuary in Maryland, USA. *Estuarine Coastal and Shelf Science* 17, 555–570.
- Zabawa, C.F., Schubel, J.R., 1974. Geologic effects of Tropical Storm Agnes on upper Chesapeake Bay. *Maritime Sediments* 10, 79–84.
- Zhong, L.J., Li, M., 2006. Tidal energy fluxes and dissipation in the Chesapeake Bay. *Continental Shelf Research* 26, 752–770.